Optimization of semi-empirical mass formula based on experimental and microscopic theoretical data

A Dissertation

Submitted in Partial Fulfillment of the Requirement for the Award of Degree of

Master of Science

In

Physics

Submitted By:

Nitika

Roll No. 302004011

Under the supervision of:

Dr. Manoj K. Sharma

Professor

TIET Patiala

THAPAR INSTITUTE
OF ENGINEERING & TECHNOLOGY
(Deemed to be University)

SCHOOL OF PHYSICS AND MATERIAL SCIENCE

THAPAR INSTITUTE OF ENGINEERING AND TECHNOLOGY, PATIALA

PUNJAB-147004

JUNE-2022

Dedicated to My Family,

My Strongest Support.

Declaration

I hereby declare that the dissertation entitled " **Optimization of semi-empirical mass formula based on experimental and microscopic theoretical data**" is an authentic record of my work carried out as requirement for the the award of the degree of **Master of Science** at **Thapar Institute of Engineering and Technology, Patiala** under the supervision of **Dr. Manoj K. Sharma**, Professor, School of Physics and Materials Science, Thapar Institute of Engineering and Technology, Patiala. No part of the matter embodied in this dissertation has been submitted to any other university or institute for the award of any degree.

Nitika

Dated: 21/07/2022

(Nitika)

302004011

It is certified that the above statement made by the student is correct to the best of my knowledge and belief.

21/07/2022

(Dr. Manoj K. Sharma)

Supervisor

Professor

TIET, Patiala

Acknowledgment

I would like to acknowledge and give my warmest thanks to my research supervisor **Dr. Manoj K. Sharma**, Professor, Thapar Institute of Engineering and Technology, Patiala. Foremost, I am extremly thankful to **Mr. Vishal Parmar**, research scholar, without his assistance and dedicated involvement in every step throughout the process, this dissertation would have never been accomplished. I would like to thank you very much for your support and understanding.

I am highly obliged to **Dr Kulvir Singh**, Head of Department, School of Physics and Materials Science and **Dr. Maninder Singh**, Dean of academic affair for their guidance during various stage of this work. I want to embrace this opportunity to acknowledge my gratitude towards all the faculty members of the School of Physics and Materials science who were always accessible and helpful.

(Nitika)

302004011

Contents

List of Tables

List of Figures

Abstract

In this dissertation, I have optimized the semi-empirical Bethe-Wizsacker formula using the least-square method. I have considered the optimization to be linear multiple regression problem, considering independent terms with some physical significance. The recently available experimental mass evaluations of AME2020 [Huang et al. Chin. Phys. C 45, 030002 (2021)] and microscopic theoretical estimation of the Hartree-Fock-Bogoliubov model (HFB-24) [Goriely et al. Phys. Rev. C 88, 024308 (2013)] are used for fitting the standard semi-empirical mass formula. Further improvements are made by introducing the isospin asymmetry (I) dependence of volume, surface, and curvature coefficients. The shell corrections proposed by Myers and Swiatecki are used in this work. It is observed that isospin asymmetry dependence of volume, surface, and curvature coefficients along with the shell energy, play a predominant role in the estimation of nuclear binding energy and related data. The best fit model is obtained by considering 13 parameters in the semi-empirical mass formula with a root mean square value of 1.54 MeV and 2.46 MeV while fitting with AME2020 and HFB-24 data, respectively. The neutron and proton drip lines are also explosed using the fitted semi-empirical formulas. The correlation analysis of the coefficients of various models indicates that the I^2 dependence of the volume, surface, and curvature coefficients does not correlate with the model parameters, making it difficult to constrain.

Chapter 1

Introduction and Literature Review

1.1 Introduction

Understanding an atomic nucleus and its constituents comprehensively is one of the most complicated and unresolved problems in physics. Ever since its discovery by Rutherford, Marsden, and Geiger in 1911 using the thin gold foil experiment, countless groundbreaking efforts have been made in the last century to understand the structure of the nucleus and the nucleons inside it. Unlike well-established electromagnetic force, the strong force that binds the nucleons inside the nucleus is still not fully understood. As a result, the nuclear potential, which plays the central role in understating the structure of the nucleus and related phenomenon, becomes uncertain, and the use of various approximations becomes inevitable [1]. In principle, one should use the in-situ calculations using appropriate postulates of quantum mechanics for individual nucleons inside a nucleus to study its structure structural properties and related mechanism. However, the problem becomes quite complicated due to its many-body nature. Furthermore, Quantum chromodynamics which is the underline theory to explain the strong interaction, also diverges at a large distance or at low energy regime [2]. Due to this, nuclear physicists often use nuclear models based on the observations combined with experience from molecular theory to understand the various properties related to the nucleus such as its structure [3], reaction [4], decay [5], etc.

One of the principal properties associated with the nucleus is its mass and binding energy. The accurate measurement of the binding energy of a nucleus is important for various phenomena related to a nucleus, such as studying the nuclear reaction mechanism [6], nucleosynthesis [7] of elements , structure of astrophysical objects [8], simulating supernova explosion [9], etc. Several state-of-the-art facilities using either the mass or energy spectrometry [10] (Liontrap at Mainz, Pentatrap at Heidelberg and Fsu-Mit-Trap at Florida, Mistral at Cern, Cyclotron time-of-flight mass spectrometry at Sara-Grenoble

and at Css2-Ganil, IUAC at Delhi [1]) across the globe are used to measure the binding energy with more and more accuracy. The principal aim of these facilities is to measure the mass of the nuclei with high isospin asymmetry [2, 11, 12, 13]. The binding energies of nuclei are updated from time to time in the form of Atomic Mass Evaluations [2]. The recent measurement completed in the AME-2020[14] table has 777 additional new experimental inputs compared to the previous data of AME-2016[15]. However, the experimental evaluations are still limited, particularly in context of the binding energy of highly asymmetric nuclei which is an important tool for various astrophysical as well as terrestrial application [16].

On theoretical front, there have been continuous efforts to construct a subtle nuclear mass model which is not too complicated yet possesses the necessary physics to measure the nuclear binding energy. The development of nuclear mass model started from the pioneering work of Weizsäcker who proposed the Semi Empirical Mass formula (SEMF) based on the liquid drop model by George Gamow [17]. The simplicity of this model still makes it one of the most used models in light of sophisticated formalisms that include microscopic framework such as Relativistic mean-field theory [18], Hartree-Fock-Bogoliubov (HFB)[19] framework or ab inito method such as Chiral Effective field theory[20], Green's Function Monte Carlo (GFMC)[21], etc. A simplistic nuclear mass-model that has high efficiency , less computational requirement and address the adequate physics of a nucleus is of great interest to physicists working in related subject domain.

1.2 Nuclear Binding Energy

The nuclear binding energy, which is the energy required to break the nucleus into its constituents, stems from the nuclear force binding the nucleons inside a nucleus. Just like molecular Van der Waals force, nuclear force also has an attractive tail. The attractive binding force thus results in the lower energy/mass of the bound system as compared to its constituents in accordance with the special theory of relativity. The difference between the masses of the constituent particles and the actual mass of the nucleus is defined as mass defect and energy as binding energy. This nuclear binding energy is million times higher than the electronic binding energy. This fact is utilized to create the cleanest form

[1] https://en.wikipedia.org/wiki/List_of_accelerator_mass_spectrometry_facilities
[2] https://www-nds.iaea.org/amdc/

of energy using nuclear fission process. However, work is also under process to develop fusion reactor as well [3].

Unlike its molecular counterpart, the nuclear force has complex nature and therefore, the accurate theoretical estimation of nuclear binding energy remains an uphill task. On the experimental front, in recent years, the measurement of Binding energy has been steadily improved by developing experimental equipments in CERN [22] and HIRFLCSR [23]. With the large-scale use of accelerator facilities, it is possible to reach near a few hundred GeV/Nucleon of center mass energies, which enables one with either a fixed-target accelerator or a collider beam to explore unknown areas of nuclear phenomena. Near the drip line, it is still tricky to find (directly or indirectly) masses of the unstable nuclei. For example, the masses of those nuclei are still experimentally unknown, which are involved in the process of capturing fast protons (rps) [24] and fast neutrons (r) [25]. Due to these factors, the theoretical mass models are urgently needed to provide highly reliable and accurate predictions for these unknown regions and the variations involved.

1.3 Nuclear mass model

In the absence of any fundamental theory to explain exact nature of nuclear force, one may use various forms of models based on certain approximations, to estimate the mass and energy of nucleus. These models usually known as the nuclear mass model are generally a function of number of nucleons and attempt to describes the theory behind the functioning and structure of the nucleus [26]. Each model is based on the resemblance analogy that makes the correlations between a large amount of the information and further helps to study of properties of the nucleus. Although continuous efforts have been made in the last century to fine tune the nuclear models, the accuracy in the calculations of the ground-state masses, deformation in the nucleus, etc., is still a massive challenge for nuclear physicist. In literature, there are various forms of mass models that have been developed in the last century. These mass models are broadly classified into two main categories i.e. macroscopic mass models and microscopic mass models. The macroscopic mass models take into account the global properties such as volume, surface, Coulomb effect of a nucleus into account. These types of models employ the molecular analogy to

[3] https://www.iter.org/mach/Tokamak

a nucleus and are able to define various global properties of the nuclei like binding energy, nucleon distribution, size, shape, etc. The microscopic models on the other hand consider individual nucleon in the nucleus and solve the respective Schrodinger or Dirac equations. The models can be of in-situ type like Green's Function Monte Carlo (GFMC) [21] or based on mean field approximation like self consisten Hartree-Fock-Bogoliubov [27, 28] and Relativistic mean field models [3]. Various combination of these methods produce various mass models such as Finite Range droplet models (FRDM) [29], Duflo and Zuker (DZ) [30], Koura et al. (KTUY) [31], HN [32], INM [33], WS4+ [34], Thomas-Fermi model (TF) [35], etc. Majority of these models explain the nuclear mass in a semi-empirical manner. In this work I attempt to optimize the parameters of the empirical formula, due to its simplicity and reliability to address basic nuclear properties.

1.3.1 Semi-empirical mass formula

To explain the properties like structure, internal motion and related complexities of nuclear system, American physicist Russian-born George Gamow formulated the liquid drop Model (LDM) in 1929, suggesting that the nucleus resembles a molecule of a droplet. This analogy is based on several identical properties of nucleus and droplet; a droplet and nucleus are mostly spherical, with Symmetrical surface tension acting toward the center. The Van Der Waals and nuclear force, which are governing force in the case of the droplet and nucleus, respectively have the same qualitative nature. The droplet releases the heat as the nuclei emit the radiation. Nuclear fission, in the case of nuclei resembles the breaking of the droplet. Some essential assumption $R \approx A^{1/3}$ is taken because the nucleus is considered as incompressible matter. This was further modified as a Semi-Empirical Mass model by C.F Von Weizsacker. The formula is based partly on theory and partly on empirical estimation. Bethe-Weizsacker mass formula was mainly designed to find the gross features of the binding energy of nucleus of higher and medium mass nuclei but fails for the lighter nuclei and the nuclei which are away from the stability line. It is relevant to note that shape and structure of the light nuclei are quit complex (loosely bound nuclei, halo nuclei, etc.) and hence estimation of nuclear behaviour becomes quite complex.

With the most simplistic terms, the semi-empirical formlula of Bethe and von Weizsacker [17, 36] is although a powerful formula yet needs modification to make it more precise. There have been several modification of this formula over the years which use

various combinations of microscopic-macroscopic properties of a nucleus [21, 37, 38, 39, 40, 41, 42, 43, 44, 45, 46]. The principle aim of these modifications are multi-fold such as (i) reducing the error compared to the experimental estimation of binding energy. (ii) making the adjustable parameters as constrained as possible etc.

In this work I have made few modifications in the parameter of semi-empirical mass formula. As suggested by [45, 46, 47, 48, 49, 50, 51], the macroscopic energy such as volume and surface should change with the isospin content of a nucleus based on various experimental and theoretical observations. Therefore, I have made the volume and surface coefficient isospin dependent up to the second order. Furthermore, for better estimation of surface energy which plays an important role on various nuclear problems such as neutron star crust physics [16], I have used the curvature energy term which is isospin dependent. The formulation is discussed in next chapter.

Chapter 2

Formulation and Methodology

2.1 The semi-empirical mass formula (SEMF)

The semi-empirical mass formula pioneered by C.F Von Weizsacker in 1935 is one of the most lucid formulas in nuclear physics. Although elementary, classical, empirical, and simple, the semi-empirical formula contains the essential physics of an atomic nucleus. A suitable calibration of its coefficient estimates binding energies of nuclei suitable for practical purposes such as studying the nuclear reaction dynamics, its structure, and a few astrophysical problems. The basic version of the formula as a function of number of protons (Z) and Mass ($A = Z + N$) is written as [17]

$$BE(Z, A) = a_v A - a_s A^{2/3} - a_c \frac{Z(Z-1)}{A^{1/3}} - \frac{a_a (N-Z)^2}{A} + \delta(Z, N). \tag{2.1}$$

Here, a_v, a_s, a_c, a_a, a_p are the coefficients of volume, surface, coulomb, symmetry and pairing energy respectively. The semi-empirical formula can be viewed as a series expansion of the $A^{-1/3}$ or R^{-1} and square of the asymmetry $(N - Z)$ terms. Such expansion is known as leptodermous expansion which takes into account the contribution of only those terms which have transparent physical meaning. The first four components of Eq. 2.1 i.e. volume, surface, Coulomb and asymmetry bear resemblance to a classical liquid-drop while the fifth pairing term corresponds to purely a quantum mechanical phenomenon.

Since the foundation of the semi-empirical mass formula resides in the assumption that nucleus is a incompressible and spherical liquid drop, it is not applicable for the nuclei in a wider mass range. With advancement in nuclear instrumentation, we know that nuclei deviate from the spherical shapes and are not completely rigid. Hence, one needs to modify the terms of the semi-empirical mass formula to make it more realistic and closer to experimental measured values.

2.2 Modified semi-empirical mass formula (M-SEMF)

To improve the performance of Eq. 2.1, we write the binding energy of a nucleus with given mass number A and proton number Z using the Strutinsky Energy Theorem [52] as

$$BE(Z,N) = BE(Z,N)_{smooth} + BE(Z,N)_{shell}, \tag{2.2}$$

where the smooth part of the binding energy [48] can be written as various combinations of following expression [47],

$$\begin{aligned} BE(Z,N) &= a_v(1-\kappa_{v_1}I-\kappa_{v_2}I^2)A + a_s(1-\kappa_{s_1}I-\kappa_{s_2}I^2)A^{2/3} \\ &+ a_{curv}(1-\kappa_{curv_1}I-\kappa_{curv_2}I^2)A^{1/3} - a_c\frac{Z(Z-1)}{A^{\frac{1}{3}}} - c_4\frac{Z^2}{A} \\ &- \delta(Z,A) - E_{shell}. \end{aligned} \tag{2.3}$$

Here isospin asymmetry | I | is given as

$$I = \frac{N-Z}{A}. \tag{2.4}$$

In Eq. 2.3, the first three terms define the volume, surface and curvature energy. The isospin dependence of these terms upto the second order is introduced to account for the asymmetric nuclear matter. These corrections help to estimate the isospin asymmetry dependent properties such as skin thickness, fission barrier etc. and give better estimation of the binding energy. These terms are also referred to malacodermous term [47]. The Coulomb energy has its standard form with a surface diffuseness correction. Pairing energy in this work have been assumed to be same for all the models and is written as [47]

$$E_{pair} = \frac{\delta(A,Z)}{A^{1/3}} = \begin{cases} +\delta_0 & Z,N \text{ even }, \\ 0 & A \text{ odd}, \\ -\delta_0 & Z,N \text{ odd}. \end{cases} \tag{2.5}$$

Finally, the shell energy which fluctuate with the mass number is taken from the

"empirical" formula of Myers and Swiatecki as [40]

$$BE(Z,N)_{shell} = C\left[\frac{F(N)+F(Z)}{(\frac{A}{2})^{\frac{2}{3}}} - cA^{\frac{1}{3}}\right] \tag{2.6}$$

where $F(X)$ is written as

$$F(x) = \frac{3}{5}\left(\frac{M_i^{\frac{5}{3}} - M_{i-1}^{\frac{5}{3}}}{M_i^{-} M_{i-1}}\right)(X - M_{i-1}) - \frac{3}{5}(X^{\frac{5}{3}} - M_{i-1}^{\frac{5}{3}}) \tag{2.7}$$

with $X = N$ or Z, $M_{i-1} < X < M_i$ and M_i 2, 8, 14 ,20, 28, 50, 82, 126 and 184 are the magic numbers for both proton and neutron. In this equation C is taken as the shell constant, and the value of c is taken as 0.26.

2.3 Linear regression and least-square fitting

Regression is the set of techniques used to establish the possible relationship between the dependent and independent variables. It is one of the most widely used statistical formulations to forecast within reasonable error intervals. Regression analysis is computationally very economical owing to its simplicity. With a careful and educated selection of dependent variables, one can bring its accuracy and predictability power at par with the available sophisticated techniques such as machine learning, neural network, etc. With a few minor extensions, it can be used to perform complex analysis among several variables. For a given vector of inputs $\mathbf{X}^T$ defined as [47]

$$\mathbf{X}^T = \begin{bmatrix} X_{0,0} & X_{0,1} & -- & X_{0,n-1} \\ X_{1,0} & X_{1,1} & -- & X_{1,n-1} \\ -- & -- & -- & X_{2,n-1} \\ X_{n-1,0} & X_{n-1,1} & -- & X_{n-1,n-1,} \end{bmatrix} \tag{2.8}$$

where T denotes the transpose, and random variable $\hat{Y}$, a regression model aims to find a likelihood function $\hat{Y} = f(\mathbf{X})$ which is the conditional distribution for $\hat{Y}$ with $\mathbf{X}$. The output of the regression model then can be written as [53]

$$\hat{Y} = \hat{\alpha_0} + \sum_{i=1}^{n} \mathbf{X}_i \hat{\alpha_i}. \tag{2.9}$$

Here, the term $\hat{\alpha}_0$ is the intercept or the bias and $\hat{\alpha}_i$ are the coefficients. For the convenience, the intercept is often absorbed in the coefficient and the resulting equation takes the simple form as [54].

$$\hat{Y} = \mathbf{X}^T \hat{\alpha}. \tag{2.10}$$

Here $\mathbf{X}^T$ is commonly known as design matrix. Often times, the functional form of $\hat{Y} = f(\mathbf{X})$ is not known and a linear relationship between dependent and independent variables is assumed. Such assumption is known as the linear regression model with $\hat{\alpha} = [\alpha_0, \alpha_1, -, -, \alpha_{n-1}]$ as the regression coefficients.

2.3.1 Optimization of regression parameters

Optimization is a process to make equation, model, etc. better by using the most effective resources. To fit the Equation of the form 2.10, I have used the method of least squares. This method is straightforward and can process large amount of data very quickly, which is our main requirement. In this approach, we minimize the residual sum of squares (RSS) which gives a measure of spread between true and parameterized value of $\hat{Y}$. The RSS(α) is a quadratic function which definitely has a minimum and is written as [55]

$$\begin{aligned} RSS(\alpha) = & \quad \tfrac{1}{N}\textstyle\sum_{i=0}^{n-1}(Y_i - \bar{Y}_i)^2 \\ = & \quad \tfrac{1}{N}(Y - \bar{Y})^T(Y - \bar{Y}) \\ = & \quad \tfrac{1}{N}(Y - \mathbf{X}\alpha)^T(Y - \mathbf{X}\alpha). \end{aligned} \tag{2.11}$$

To find the coefficients we then minimize

$$\underset{\alpha \in R}{\text{MIN}} \frac{1}{N}(Y - \mathbf{X}\alpha)^T(Y - \mathbf{X}\alpha), \tag{2.12}$$

to get the unique solution as [55]

$$\hat{\alpha} = (\mathbf{X}^T\mathbf{X})^{-1}\mathbf{X}^T y. \tag{2.13}$$

It is necessary that the product $\mathbf{X}^T\mathbf{X}$ is non-singular. For an optimized set of coefficients, the goodness of the optimization can be determined using following tools.

2.3.2 Mean absolute error

The mean absolute error is defined as the average of the absolute error among the observed and the calculated data. This can be written as

$$\mathbf{MAE} = \frac{1}{n}\sum_{i=1}^{n}|X_i - \hat{X}_i| \tag{2.14}$$

where, $\hat{X}_i$ is the observed value with respect to the experimental value X_i and n is the sample size.

2.3.3 Root mean square error (RMSE)

Root mean square error is the error which is commonly used in the calculation of the differences between predicted and observed values (sample or population values) by an estimator or model. Mathematically it is defined as the square root of the mean square error. It is written as

$$RMSE = \sqrt{\frac{1}{n}\sum_{i=1}^{n-1}(X_i - \hat{X}_i)^2}, \tag{2.15}$$

where, $\hat{X}_i$ is the observed value with respect to the experimental value X_i and n is the sample size. RMSE is usually preferred over the MAE because RMSE measures the same unit as the output variable, although MAE measures the squared unit of the output variable. The least value of the RMSE is considered to be the best, because one can get to know the deviation in predicted value to the actual value.

2.3.4 R2 score

R2 score is the amount of dissimilarity in the output value that is predicted from the input values. It is also known as the coefficient of determination. It plays the vital role in describing the model's goodness of fit, and describe the accuracy of predicted data. R2 score is given as

$$R2 = 1 - \frac{\sum_{i=i}^{n}(X_i - \hat{X}_i)^2}{\sum_{i=i}^{n}(X_i - \bar{\hat{X}}_i)^2}, \tag{2.16}$$

where $\hat{X}_i$ is the observed value with respect to the experimental value X_i. The best possible R2 score is 1.0, and it can be negative because of the arbitrarily worse model.

R2 score is 0.0 for the constant model as the input features are neglected.

2.4 Correlation

For the relationship between two-dimensional random variables, x and y, the covariance of the sample can be given as

$$\bar{w}_{xy} = \frac{1}{n-1}\sum_{i=1}^{n}(x_i - \bar{x})(y_i - \bar{x}) \tag{2.17}$$

The correlation coefficient is then written as

$$C = \frac{w_{xy}}{w_x w_y} \tag{2.18}$$

where w_{xy} and C are defined as the measurement of the interrelation between x and y. If the value of the correlation is positive, it means that the value of both variables is in the same direction. If the value of the correlation is negative, it means the value of one of the variables is increasing and another variable value is decreasing. If the variables are nonrelated to each other, the correlation value can be neutral or zero.

2.5 Separation Energy

Separation energy is defined as the energy that is required to remove nucleon (proton or neuron) from the atomic nucleus. The usual accepted method to find the separation energy for the one neutron separation energy can be written as [56]

$$SE_n = -\mathbf{Q}_n = BE(N,Z) - BE(N-1,Z) \tag{2.19}$$

BE(N-1,Z) is final (removal of one neutron) binding energy of nucleus. One proton separation energy can be given as

$$SE_p = -\mathbf{Q}_p = BE(N,Z) - BE(N,Z-1) \tag{2.20}$$

BE(N,Z-1) is final (removal of one proton) binding energy of nucleus.Two neutron separation energy can be given as

$$SE_{2n} = -\mathbf{Q}_{2n} = BE(N, Z) - BE(N-2, Z) \tag{2.21}$$

BE(N-2,Z) is final (removal of two neutron) binding energy of nucleus respectively. Two proton separation energy can be given as

$$SE_{2p} = -\mathbf{Q}_{2p} = BE(N, Z) - BE(N, Z-2) \tag{2.22}$$

BE(N,Z-1) is final (removal of two proton) binding energy of nucleus.
The results obtained is discussed in the next chapter.

Chapter 3

Results and discussion

In this work, I attempt to optimize various nuclear mass models of semi-empirical macro-microscopic nature to estimate the binding energy of a nucleus with a given mass number (A) and proton number (Z). The aim here is to propose a semi-empirical formula that is simplistic, efficient and take minimal computational resources. I start with the basic semi-empirical formula with five standard terms, i.e., volume, surface, Coulomb, asymmetry, and pairing. I optimize the relevant coefficients of this formula to reproduce the binding energy of two separate mass evaluations, which are 1) experimental mass evaluation of AME2020 [14] and 2) theoretical microscopic evaluation of Hartree-Fock-Bogoliubov (HFB-24)[57], which is estimated using the well calibrated BSK Skyrme functional [58]. The HFB approach is believed to be precise and is used in various studies of neutron-rich nuclei [57, 59]. The semi-empirical formula is then modified by including various physical effects such as the effect of isospin asymmetry on bulk properties and the inclusion of curvature effects. Several forms of the modified semi-empirical are fitted on the experimental data of AME2020 [14] and microscopic theoretical calculation of Hartree-Fock-Bogoliubov (HFB 24) [19]. Publicly available scikit-learn[1] python library along with the SciPy [2] optimization algorithm is used in this work. These tools are one of the most efficient and commonly used libraries in predictive analysis. In the following sections, I will discuss the optimization of the mass models in detail.

3.1 Semi-empirical mass formula (SEMF)

I begin my optimization with the semi-empirical mass formula given by Eq. 2.1. To optimize the coefficients of the model to give the least value of RMSE, the standard multiple linear regression algorithm involving least square method is used (described in section 2.3). I have cross-checked the goodness of the fit with other optimization

[1] https://scikit-learn.org/stable/
[2] https://scipy.org/

Table 3.1: Coefficient of the semi-empirical formula (2.1) using experimental data of AME2020. The RMSE error is 3.61, MAE is 2.52 and R2 score is 0.99.

Coefficient (MeV)		Confidential Interval			
		95%		99%	
a_v	15.229	15.167	15.291	15.150	15.308
a_s	15.968	16.160	15.776	16.213	15.723
a_c	0.682	0.687	0.678	0.688	0.677
a_a	22.250	22.405	22.095	22.448	22.052
a_p	12.028	9.668	14.388	9.012	15.045

Table 3.2: Coefficient of the semi-empirical formula (2.1) using Microscopic theoretical estimation of HFB-24. The RMSE error is 6.05, MAE is 4.64 and R2 score is 0.99

Coefficient (MeV)		Confidential Interval			
		95%		99%	
a_v	14.866	14.837	14.8950	14.828	14.904
a_s	14.053	13.961	14.145	13.932	14.173
a_c	0.678	0.676	0.680	0.675	0.681
a_a	22.330	22.280	22.3795	22.264	22.395
a_p	11.872	9.762	13.982	9.098	14.646

algorithms, which uses more complicated procedures such as ridge regression [60] and found that the accuracy is not affected significantly. Therefore, the least square method is used for all the optimizations in this dissertation. Furthermore, I use the pandas data-frame [3] library due to its effectiveness in handling and processing large data.

The coefficients of the semi-empirical formula (Eq. 2.1) are given in Table 3.1 and Table 3.2 fitted on the latest available experimental mass evaluations of AME2020 and microscopic theoretical estimation of HFB-24 respectively. The HFB24 estimations of nuclear mass are used, as they are important in the large isospin regime unlike experimental evaluation which have maximum isospin of ≈ 0.3. I have taken all 2461 experimentally measured masses of AME2020, omitting the ones that have been interpolated/extrapolated theoretically and 8441 evaluations of HFB-24. I also provided the 95% and 99% confidence intervals of the coefficients to assess the statistical significance of these coefficients. It is desired that the range of the confidence interval is as narrow as possible for a given parameter. One can see that among all the coefficients, the Coulomb term is the most constrained while the pairing have the largest spread in both Table 3.1 and Table 3.2. However, all the coefficients are statistically significant as there is not a large spread in their values for these confidence intervals. This further advocated that all

[3] https://pandas.pydata.org/

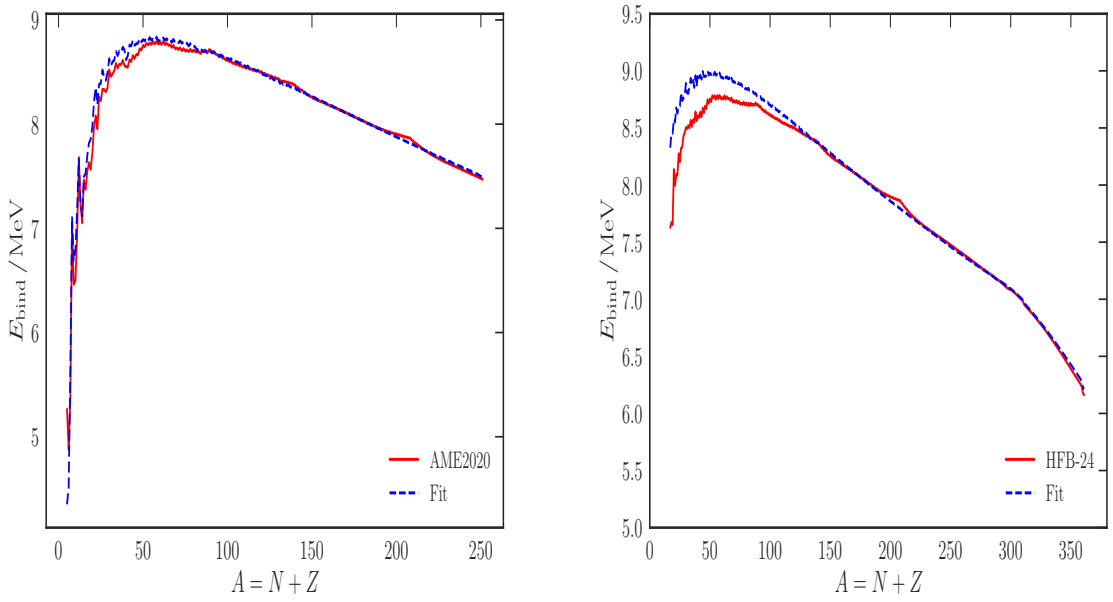

(a) (b)

Figure 3.1: Comparison of estimations of binding energy by semi-empirical formula fitted on a) experimental binding energy of AME2020 [14] and b) microscopic binding energy of HFB24 [19] for the most stable nuclei.

the physical terms in the basic semi-empirical formula have significant relevance individually. The coefficient of volume slightly decreases when one fit the Eq. 2.1 with HFB-24 data. However the oscillations among the coefficients is not significant and therefore the RMSE value of the fit is 6.035 against the 3.11 for the case of AME2020 data. This indicates an urgent need to improve the semi-empirical formula to accommodate the various structural effects such as isospin dependence of the individual component in the Eq. 2.1.

Fig. 3.1 compares the calculated binding energy of the most stable nucleus for a given mass number A with the experimental and theoretical values in the left and right panels, respectively. The fitted models, i.e., on experimental and theoretical data, seems to predict the binding energy with reasonable accuracy. It almost overlaps the experimental and theoretical values for higher mass while deviating slightly for the lighter mass region. This result is an artifact of the semi-empirical formulas [41, 47, 57, 61, 62, 63, 64, 65, 66] which indicates that the lighter mass nuclei are significantly impacted by the unrepresented structural effects in the semi-empirical formula. The deviation for the lighter mass nuclei is more significant for the HFB case as compared to the AME2020 because HFB data contains the nuclear mass for the nuclei having large mass asymmetry. The simple

semi-empirical formula such as Eq. 2.1 can not explain their binding energies.

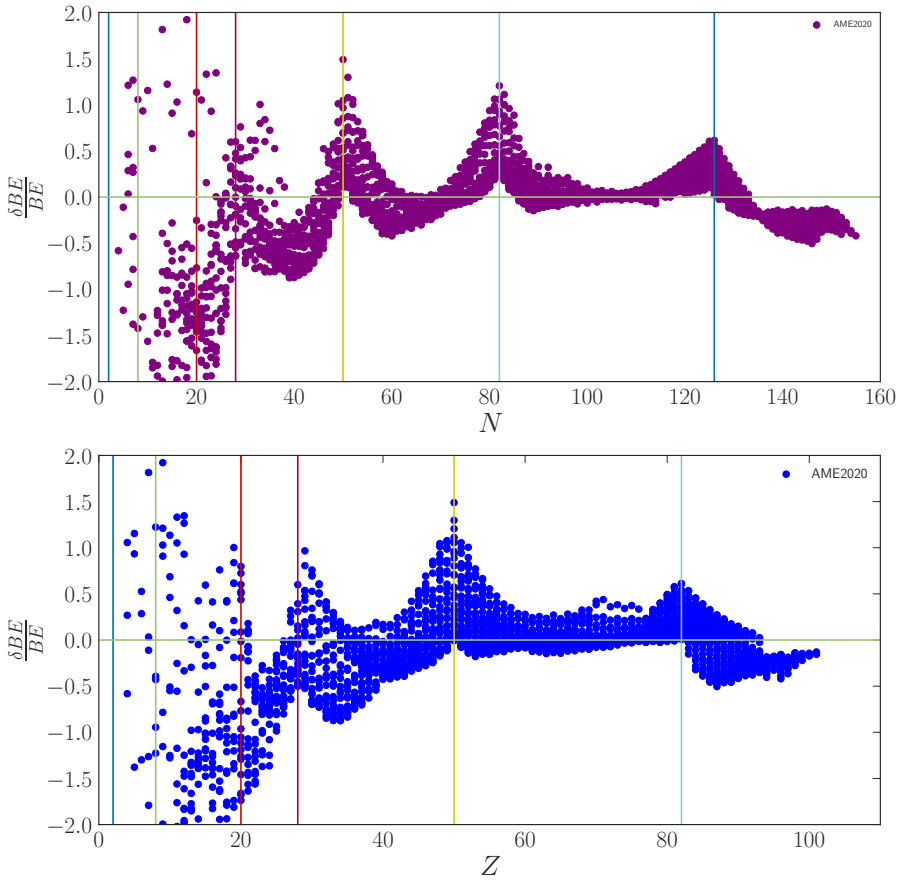

Figure 3.2: Residual of the calculated binding energy with that of experimental binding energy as a function of neutron number N in upper panel and proton number Z in the lower panel.

To analyze this further, we show the residual of the fitted semi-empirical formula in Fig. 3.2 as a function of neutron N and proton number Z for the AME2020 case. The error in the calculated binding energy is within 2%. The residual plot shows the specific pattern of peaks where the peaks can be traced to the magic number for neutron (2, 8, 20, 28, 50, 82, 126) and proton (8, 20, 28, 50, 82, 114) respectively. In general, the pattern in a residual plot suggests the need for modifications in the dependent parameters. The formation of the peaks can be understood as the result of many competing structural effects such as a) larger number of stable nuclei around the magic numbers, b) deviation of nuclei from the spherical shape, and c) impact of shell corrections. The lighter nuclei seem

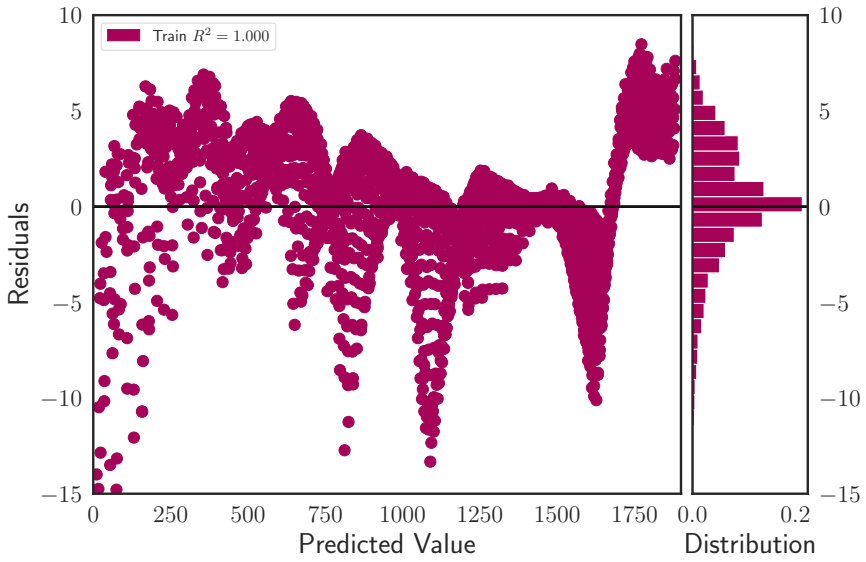

Figure 3.3: Residual bar plot the semi empirical formula fitted on AME2020 data

to show scattered residuals showing the chaotic nature of the semi-empirical formula for the lighter mass nuclei. It is evident that the formula behaves reasonably well at medium and higher mass region. The HFB-24 case yields similar qualitative results.

We have formulated our problem to be a linear multiple regression optimization. To check this basic assumption, we plot the distribution of the residual plot in Fig. 3.3. Residual plot analysis is often used to check the difference between the fitted and experimental values. This method works on the important assumption of the linear model that errors are normally distributed and are independent. The distribution in Fig. 3.3 shows that the random dispersion of the points of the residuals is around the horizontal axis, which shows that the linear regression model is suitable for the optimization of nuclear mass models.

To see the practical applicability of the model, we show in Fig. 3.4a and 3.4b the comparison of the two neutrons and proton separation energy calculated using the fitted formula 2.1 and combined with the experimental binding energy data. The separation energies estimated from the fitted formula seem to be quite accurate, almot at par with the experimental data.

We further fit the Eq. 2.1 on other available atomic mass evaluations from experiments , i.e., AME2020 [14], AME2016 [15], AME2012 [67], AME2003 [66], and microscopic theoretical calculations, i.e., HFB-24 [59] and HFB-26 [59]. The evaluated coefficients are

Table 3.3: Coefficients calculated in this work by using different experimental and microscopic data

data	a_v (MeV)	a_s (MeV)	a_c (MeV)	a_a (MeV)	a_p (MeV)
AME2020	15.22	15.96	0.68	22.25	12.02
AME2016	15.31	16.25	0.68	22.47	11.76
AME2012	15.25	16.06	0.68	22.32	11.14
AME2003	15.23	15.97	0.68	22.25	12.01
HBF24	14.86	14.05	0.67	22.33	11.87
HFB26	15.17	15.47	0.69	22.84	11.37

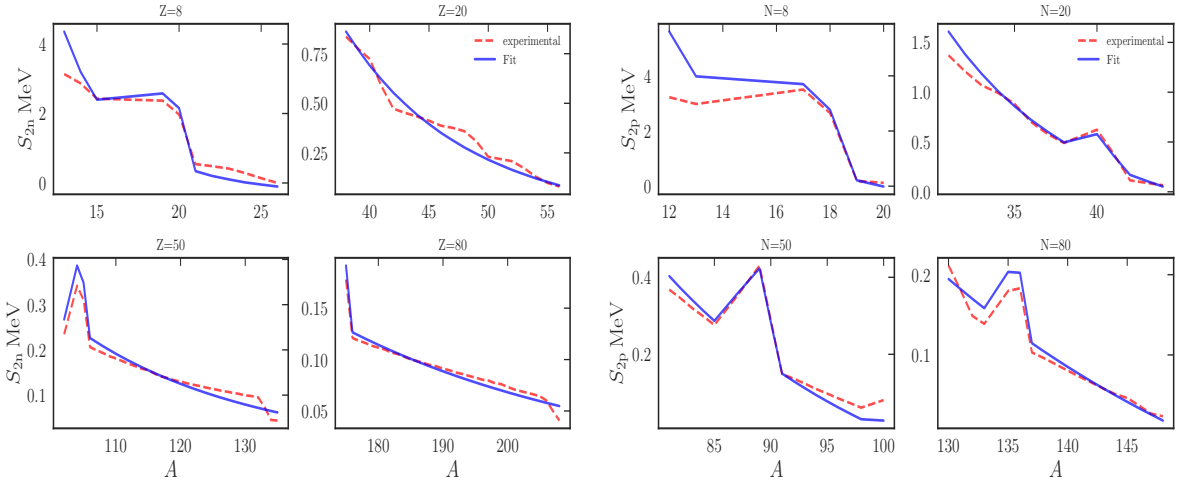

(a) (b)

Figure 3.4: Comparison of experimental (AME2020) two neutron and two proton separation energy per nucleon with respect to the fitted separation energy using eq. 2.22 and 2.21.

given in Table 3.3. It is seen that the Coefficient for the Coulomb term is constrained tightly, giving similar values for all the fittings. The volume term remain $\approx$ 15 MeV and pairing term $\approx$ 22 MeV. The HFB-24 and HFB-26 cases have a larger RMSE compared to the AME results. This is due to the fact that HFB data contain nuclei with higher asymmetry; hence, a simple semi-empirical formula might not apply in that regime. All the five coefficients in the semi-empirical formula do not oscillate much when fitted with different mass evaluations. Therefore, there is a need to introduce new parameters in the model.

The above analysis shows that the semi-empirical formula with five standard terms is quite accurate and can quantify the binding energy consistent with the corresponding experimental values. The approximated simple linear regression method seems to be

a good approximation. However, refining the semi-empirical formula and reducing the RMSE and discrepancies at the lower mass regime is still necessary. For this, we consider a modified form of the semi-empirical formula in the following section.

3.2 Modified semi-empirical formula (M-SEMF)

The standard semi-empirical formula in the section above considers the static value of the coefficient, i.e., independent of the mass number A and proton number Z. However, it is intuitive that the coefficient, such as volume and surface, should change with the nucleus. For example, the volume energy of symmetric infinite nuclear matter is different from that of asymmetric nuclear matter (the volume energy in the semi-empirical formula is that of infinite nuclear matter) [2, 68]. Therefore, we consider a few modifications in the semi-empirical formula keeping in mind that the simplicity and efficiency of the model are not compromised. Furthermore, only leptodermous terms are considered because each term in the model should have a physical relevance and consequently can be constrained based on theoretical and experimental observations. In principle, one can have an infinitely large number of terms in the mass model to accommodate all the structural effects. However, one might find the terms statistically uncertain (or impossible to constrain). One such example is the famous Duflo-Zuker mass formula with 13 and 31 parameters [30] including microscopic corrections. This formula is quite efficient but suffers from the fact that all the parameters of the model are not possible to constraint. The mostly used finite range liquid drop model (FRDM) [44] is also a powerful formalism in terms of its predictive power but is quite complicated and require a lot of computational power when applied for practical purposes (say reaction dynamics). Therefore, we consider a formula as given in Eq. 2.3 which is simple and optimize it on the available binding energy data. The main ingredient of the Eq. 2.3 is that it take into account the isospin dependence of volume, surface and curvature terms upto second order. The curvature term is introduced taking motivation from [69] to account for the local curvature of the nucleus. It is known to give a better description of surface energy of nuclei [16].

Table 3.4: Parameter of Modified Semi-empirical mass formula (M-SEMF) (Eq. 2.3) fitted using the experimental Mass Evaluations (AME2020 [14]) data. The radius of the nuclei is calculated by $r_0 = 3e^2/5a_c$ [47]

Sr.No.	a_v (MeV)	κ_{v1} (MeV)	κ_{v2} (MeV)	a_s (MeV)	κ_{s1} (MeV)	κ_{s2} (MeV)	a_{curv} (MeV)	κ_{curv1} (MeV)	κ_{curv2} (MeV)	c_4 (MeV)	a_c (MeV)	pair (MeV)	r_0 (fm)	shell (MeV)	MAE (MeV)	RMSE (MeV)
1	15.19	-	1.45	15.87	-	-	-	-	-	-	0.67	11.98	1.27	no	4.63	3.60
2	15.16	-	1.40	16.43	-	-	-	-	-	-0.91	0.69	11.57	1.25	no	2.46	3.54
3	14.21	-	1.46	9.93	-	-	10.49	-	-	-	0.64	11.70	1.32	no	2.42	3.49
4	14.34	-	1.42	11.21	-	-	8.90	-	-	-0.62	0.65	11.45	1.32	no	2.39	3.46
5	15.80	0.16	1.19	18.51	0.43	-	-	-	-	-0.70	0.70	11.27	1.22	no	2.13	2.96
6	14.86	-	1.46	12.48	-	-1.29	9.14	-	8.28	-	0.67	11.66	1.27	no	2.09	2.79
7	17.71	0.29	1.08	32.13	0.82	-	-21.77	1.25	-	-2.22	0.78	11.04	1.10	no	2.05	2.71
8	18.27	0.34	1.02	32.13	0.82	-	-21.77	1.25	-	-	0.78	11.04	1.10	no	2.05	2.71
9	16.47	0.102	1.56	18.96	0.012	1.53	-	-	-	1.42	0.72	10.95	1.19	no	1.93	2.53
10	18.8	-	1.71	20.64	-	1.13	-2.74	-	0.24	-2.10	0.73	10.95	1.17	no	1.92	2.52
11	16.87	0.93	1.57	23.22	0.027	1.45	-6.60	-0.48	1.89	-	0.75	11.00	1.15	no	1.92	2.51
12	17.17	0.12	1.52	23.22	0.02	1.46	-6.60	-7.09	1.89	1.18	0.75	11.00	1.15	no	1.92	2.51
13	15.20	-	1.40	16.48	-	-	-	-	-	-	0.68	11.76	1.27	0.61	1.96	2.93
14	15.20	-	1.40	16.48	-	-	-	-	-	-0.89	0.69	11.37	1.25	0.61	1.88	2.86
15	14.30	-	1.46	10.29	-	-	9.95	-	-	-	0.64	11.50	1.33	0.60	1.87	2.81
16	14.43	-	1.42	11.57	-	-	8.37	-	-	-0.61	0.65	11.27	1.31	0.60	1.82	2.77
17	16.39	0.15	1.49	19.44	0.29	1.26	-	-	-	0.77	0.71	11.41	1.20	0.34	1.67	2.20
18	15.82	0.16	1.19	18.47	0.41	-	-	-	-	-0.50	0.70	11.10	1.71	0.59	1.45	2.18
19	14.84	-	1.37	12.08	-	-2.26	10.01	-	9.01	-	0.67	11.43	1.27	0.60	1.45	1.87
20	17.68	0.27	1.09	31.51	0.76	-	-20.77	1.15	-	-2.041	0.78	10.90	1.10	0.57	1.31	1.86
21	18.19	0.32	1.03	31.51	0.76	-	-20.77	1.15	-	-	0.78	10.90	1.10	0.57	1.31	1.86
22	15.78	-	1.62	19.58	-	0.90	-0.98	-	-22.14	-1.89	0.73	10.81	1.18	0.58	1.17	1.55
23	16.65	0.08	1.49	21.80	0.05	0.87	-4.35	-0.35	3.08	-	0.74	10.84	1.16	0.58	1.16	1.54
24	16.89	0.11	1.45	21.80	0.05	0.87	-4.35	-0.35	-3.07	0.95	0.74	10.84	1.15	0.58	1.16	1.54

Table 3.5: Parameter of Modified Semi-empirical mass formula (M-SEMF) (Eq. 2.3) fitted using the microscopic Mass Evaluations (HFB24 [59]) data. The radius of the nuclei is calculated by $r_0 = 3e^2/5a_c$ [47]

Sr.No.	a_v (MeV)	κ_{v1} (MeV)	κ_{v2} (MeV)	a_s (MeV)	κ_{s1} (MeV)	κ_{s2} (MeV)	a_{curv} (MeV)	κ_{curv1} (MeV)	κ_{curv2} (MeV)	c_4 (MeV)	a_c (MeV)	pair (MeV)	r_0 (fm)	shell (MeV)	MAE (MeV)	RMSE (MeV)
1	14.86	-	1.50	14.05	-	-	-	-	-	-	0.67	11.81	1.27	no	4.67	6.03
2	14.63	-	1.53	12.59	-	-	-	-	-	1.08	0.64	11.73	1.35	no	4.43	5.78
3	13.29	-	1.59	1.18	-	-	30.34	-	-	-	0.63	12.01	1.35	no	3.34	4.48
4	12.64	-	1.67	-3.47	-	-	35.58	-	-	1.80	0.58	11.95	1.47	no	2.56	3.51
5	15.19	0.20	1.31	18.87	0.70	-	-	-	-	-0.34	0.70	11.72	1.23	no	2.48	3.33
6	17.36	0.37	1.20	32.88	1.420	-	-27.20	2.65	-	-2.38	0.74	11.51	1.16	no	2.09	2.78
7	17.96	0.43	1.13	32.88	1.42	-	-27.20	2.65	-	-	0.74	11.51	1.15	no	2.09	2.78
8	14.03	-	1.74	6.93	-	2.53	19.83	-	0.09	-	0.64	11.75	1.33	no	1.96	2.72
9	14.62	-	1.75	11.20	-	2.03	22.77	-	0.34	-0.91	0.68	11.69	1.26	no	1.92	2.63
10	16.48	0.15	1.49	19.73	0.28	1.16	-	-	-	0.77	0.72	11.62	1.19	no	1.90	2.56
11	17.01	0.24	1.39	25.14	0.79	0.71	-10.76	2.49	0.03	-	0.73	11.56	1.18	no	1.87	2.52
12	16.94	0.23	1.40	25.14	0.79	0.71	10.76	2.49	0.03	-0.26	0.73	11.56	1.17	no	1.87	2.52
13	14.84	-	1.50	13.97	-	-	-	-	-	-	0.67	11.51	1.27	0.46	4.39	5.76
14	14.59	-	1.53	12.43	-	-	-	-	-	1.13	0.64	11.42	1.35	0.48	4.17	5.48
15	13.31	-	1.59	1.38	-	-	29.71	-	-	-	0.63	11.75	1.35	0.40	3.09	4.20
16	12.64	-	1.67	-3.36	-	-	35.031	-	-	1.84	0.58	11.67	1.48	0.45	2.29	3.09
17	15.84	0.19	1.31	18.58	0.69	-	-	-	-	-0.28	0.70	11.48	1.23	0.38	2.21	2.99
18	17.25	0.38	1.18	28.62	1.45	-	-20.24	3.20	-	-	0.72	11.34	1.19	0.34	1.85	2.47
19	16.79	0.34	1.24	28.62	1.45	-	-20.24	3.20	-	-1.85	0.72	11.34	1.20	0.35	1.85	2.47
20	14.46	-	1.73	10.09	-	1.86	15.24	-	0.69	-0.68	0.67	11.48	1.28	0.36	1.71	2.36
21	14.02	-	1.72	6.88	-	2.14	19.82	-	0.94	-	0.64	11.51	1.33	0.38	1.76	2.29
22	16.39	0.15	1.49	19.44	0.29	1.12	-	-	-	0.77	0.71	11.41	1.20	0.34	1.67	2.20
23	16.24	0.19	1.43	20.46	0.80	0.59	-3.03	7.78	-4.53	-	0.71	11.38	1.21	0.34	1.65	2.16
24	16.27	0.20	1.43	20.46	0.80	0.59	-3.036	7.78	-4.53	0.13	0.73	11.38	1.17	0.34	1.65	2.16

In order to identify a model with best fit and study its implications, I take various combination of the coefficent in Eq. 2.3 and fit them based on a) microscopic binding energy from AME2020 and b) microscopically estimated binding energy using HFB-24. Both the mass tables differs in terms of number and nature of the nuclei. The HFB-24 data comprises nuclei with extreme isospin while the AME2020 data has maximum isospin of ≈ 0.3. The values of the coefficients are given in Table 3.4 for the models which are fitted with the AME2020 data and Table 3.5 for the models which are fitted with the HFB-24 data. We have used the shell correction term from the Myers and Swiatecki model [52]. It is relevant to mention here that the coefficient C of the Myers and Swiatecki Eq. 2.6 is also fitted along with the rest of the terms to get the least value of RMSE. The common observations by inspecting the Table 3.4 and Table 3.5 are as follows.

- The coefficient of surface diffuseness energy (C_4) does not have a significant role in estimating the binding energy. This fact is visible by comparing the RMSE of models No. 11 and 12 in Table 3.4 and Table 3.5. The RMSE does not change when fitting the model with or without the C_4. This result is consistent with the [47].

- The inclusion of curvature energy lowers the RMSE to ≈ 0.04 MeV (see model 9 and 12 in Table 3.4 , 10 and 12 in Table 3.5). It influences the fitting results for the case of HFB-24 more significantly. This may be due to the fact that curvature effects become important for the nuclei having larger asymmetry due to their deviation from the spherical shape. Therefore, the curvature energy is an important factor in ascertaining the binding energies in the unconventional regime of the nuclear chart.

- The $|I|$ and I^2 dependence of volume, surface, and curvature energy (so-called malacodermous terms) play a crucial role in the estimation of the binding energy of a nucleus and should be included in any mass model similar to this work. When comparing the model 1 and 12, 13 and 24 in Table 3.4 and 3.5, it is clear that $|I|$ and I^2 dependence of volume, surface, and curvature coefficients are necessary to estimate the binding energy as well as the individual energies represented by these coefficients.

- The most important aspect of Table 3.4 and 3.5 is that the pairing energy and Coulomb energy coefficient are tightly constrained i.e. they do not oscillate when

fitting various models such as in Table 3.4 and 3.5. On the other hand, coefficients of curvature energy and its $|I|$ and I^2 dependence have a large variation. The surface energy coefficient also very among the models considered in Table 3.4 and 3.5. Therefore, there is need to have a more stringent values of surface coefficient as it influence the determination of saddle-point of the potential barrier and fission properties. [2]

- The shell energy plays a predominant role in the reduction of the RMSE. It reduces the error up to 1 MeV. The simple semi-empirical formula (Eq. 2.1) with shell correction itself reduces the RMSE considerably. This reduction originates from the fact that shell energy is the oscillating part of the Eq. 2.3 and can not be explained by any other classical terms. The best-fitting result is obtained by considering all the terms of Eq. 2.3 along with the shell correction.

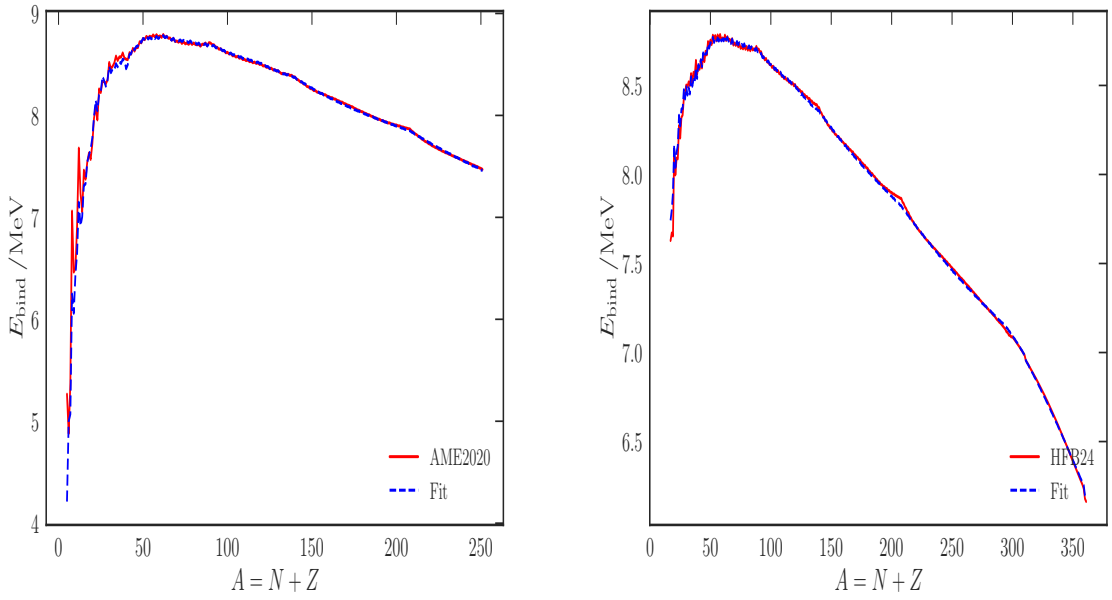

(a) (b)

Figure 3.5: Comparison of binding energy for most stable nuclei calculated by the Eq. 2.3 using the coefficients with best results and fitted with the a) experimental AME2020 and b) microscopic HFB-24 data.

Fig. 3.5 shows the comparison of the binding energy of the most stable nucleus for a given mass number. The left panel shows the results for model 24 in Table 3.4 while the right graph shows the estimations of model 24 in Table 3.5. These two models estimate

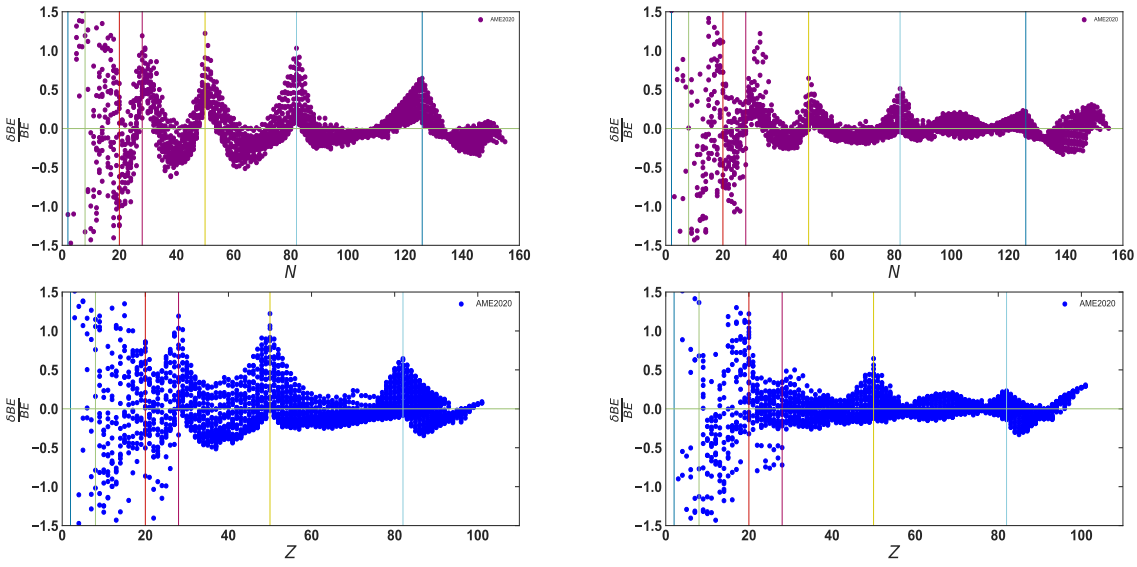

(a) (b)

Figure 3.6: Comparison of difference between the experimental data AME2020 and fitted binding energy per nucleon with respect to N neutron and Z proton .(a)graph represents difference in binding energy without shell correction.(b)graph represents difference in binding energy with shell correction.

the least value of the RMSEs. It is clear from the figure that the models are accurate for all the mass range. These models have remarkable accuracy for the higher mass region. This is clearly an improvement as compared to the Fig. 3.1 for the standard semi-empirical formula, which was not accurate for the lower mass region.

Fig. 3.6 shows the impact of including shell correction in the mass formula. The peaks around magic numbers observed in the semi-empirical formula still persist for the modified semi-empirical formula. However, the shell correction inclusion significantly reduces the height of the peaks. There is still a chaotic behavior for the nuclei in the lighter mass range. This further tells us that some effects still absent in the modified semi-empirical formula. The impact of considering only the spherical shape is also visible in the form of peaks.

The residual bar plot to show the normal distribution of the errors is shown in fig. 3.7. The residuals are normally distributed with no outliners. The inclusion of shell correction reduces the positive tail (left panel) in case of the model without shell correction. However, there are still few patterns which indicate that the model can be further refined.

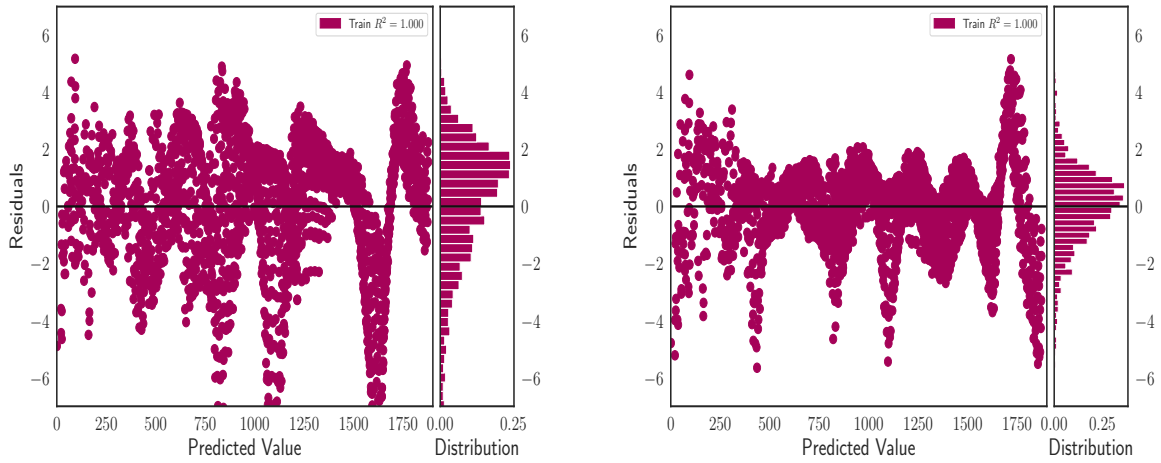

(a) (b)

Figure 3.7: Residual plot of fitted binding energy by using eq. 2.3 of data plotted wih respect to AME2020. (a) Residual plot of fitted binding energy without shell energy. (b) Residual plot of fitted binding energy with shell energy.

Apart from it, the modified semi-empirical formula with the shell effect inclusion seems to work with adequate efficiency.

Finally, to address the applicability of the models, I have calculated the two neutron and proton separation energy which is shown in Fig. 3.8. The upper panel shows the fitted model without the shell correction while the lower panel show the separation energies with shell correction. Both the models estimate the two neutron and proton separation energy consistent with the experimental estimation. The inclusion of shell corrections reduces the difference of the theoretical and experimental estimations, but is not much significant. This is due to the fact that the fitting procedure try to distribute the binding energy to the available coefficents such as volume, surface, curvature, asymmetry, shell, pairing, etc.

From the above discussions, I propose two new sets of coefficents of the mass formula i.e. Eq. 2.3 which can be applied based on the range of application. For the conventional regime i.e. with $I < 0.3$ which reproduces the experimental AME2020 data, the formula is given as

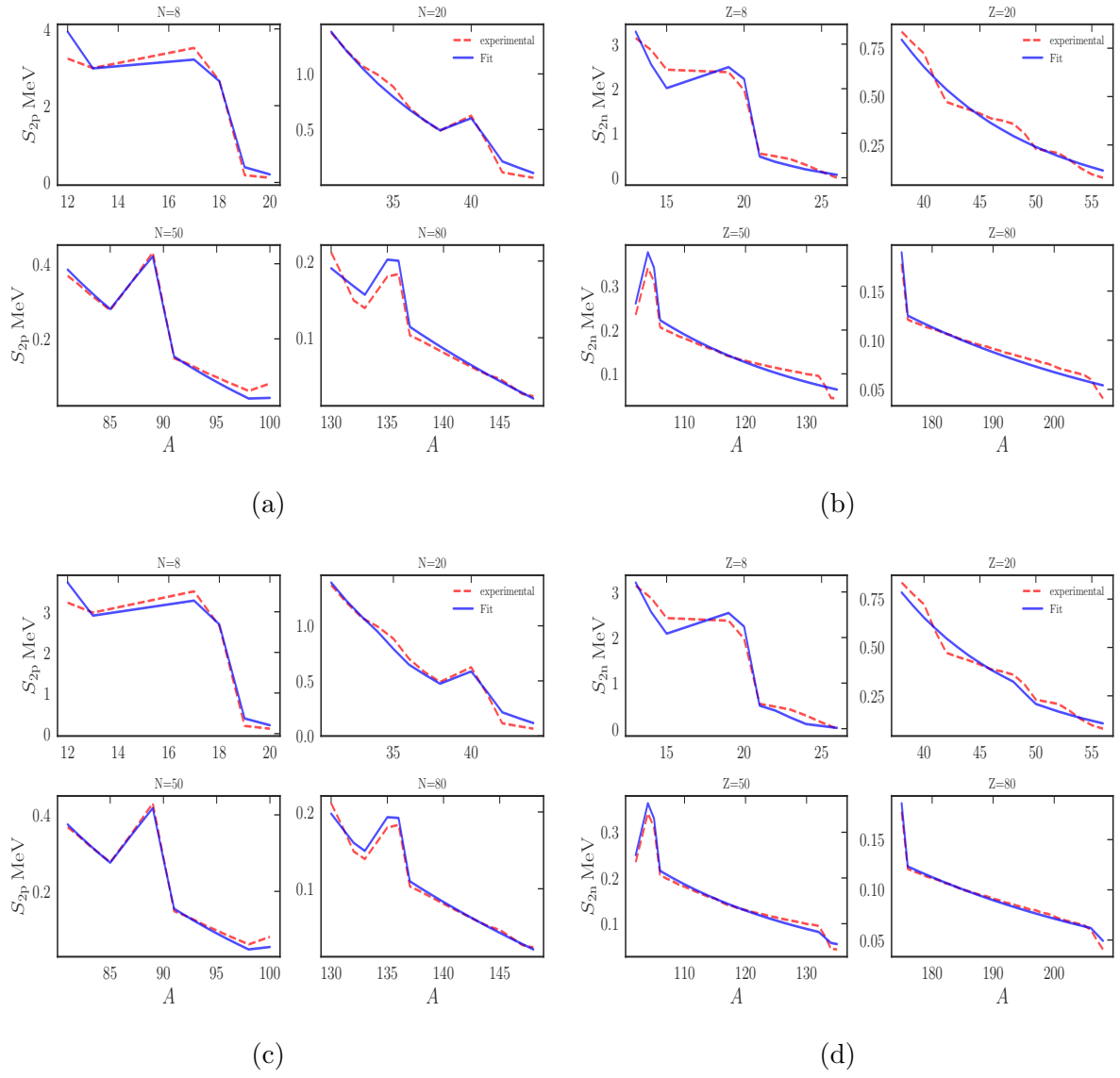

Figure 3.8: Comparison of experimental (AME2020) two neutron and two proton separation energy per nucleon for mass number Z=8, 20, 50, 80 with respect to the theoretical separation energy using eq.3.4a and 3.4b. (a) Two proton separation energy with respect to mass number without adding shell energy. (b) Two neutron separation energy with respect to mass number without adding shell energy. (c) Two proton separation energy with respect to mass number with adding shell energy. (d) Two neutron separation energy with respect to mass number with adding shell energy.

$$\begin{aligned} BE(Z,N) &= 16.89(1-0.11I-1.45I^2)A + 21.80(1-0.054I-0.87I^2)A^{2/3} \\ &- 4.35(1-0.35I-3.08I^2)A^{1/3} - 0.74\frac{Z(Z-1)}{A^{\frac{1}{3}}} \\ &- 10.84E_{pair} - 0.58E_{shell}, \end{aligned} \tag{3.1}$$

and for the case $I > 0.3$ which practically reproduces the HFB-24 data is given by

$$\begin{aligned} BE(Z,N) &= 16.27(1-0.20I-1.43I^2)A + 20.46(1-0.80I-0.59I^2)A^{2/3} \\ &- 3.036(1-7.78I-4.53I^2)A^{1/3} - 0.71\frac{Z(Z-1)}{A^{\frac{1}{3}}} \\ &- 11.38E_{pair} - 0.34E_{shell}. \end{aligned} \tag{3.2}$$

One of the most important need for an effective theoretical mass model is to determine the proton and neutron drip lines as current experimental techniques are not sufficient to explore them. I have estimate these drip lines using the optimised semi-empirical mass models. The proton and neutron drip nucleus are determined by calculating the one proton (S_p) and neutron (S_n) separation energy respectively. The configuration where S_p become positive for the first time gives the proton drip while where (S_n) become positive gives us neutron drip nucleus. In Fig. 3.9 I have shown the neutron and proton drip lines along with the most stable nuclei. The left panel shows the result using the standard and modified SEMF fitted on AME2020 data while the right panel show the result with using the MSEMF fitted on AME2020 and HFB-24 data. There is considerable difference in the SEMF and M-SEMF formula in terms of their drip lines. The M-SEMF estimate the proton and neutron drip lines at lower Z value. The M-SEMF models fitted on AME2020 and HFB-24 data however does not show much deviation while predicting the drip lines. I have used the models with least RMSE in their respective categories.

3.2.1 Correlation

In Fig. 3.10, I have shown the correlation heatmap among the parameters of the M-SEMF given by Eq. 2.3 based on the various fitted models given in Table 3.4 and 3.5. The correlation analysis of the parameters of a model is necessary to study the inter-dependency which might influence the efficiency of the fitted model. The available correlations are

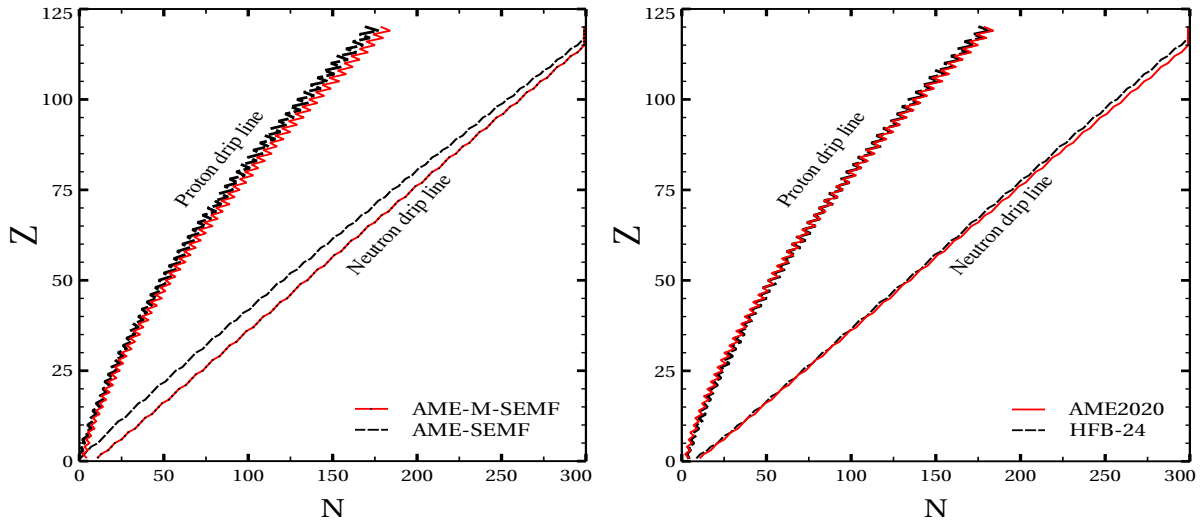

Figure 3.9: The proton and neutron drip lines calculates using the a) SEMF and M-SEMF models fitted on AME2020 data and b) M-SEMF models fitted on AME2020 and HFB-24 data. We use the models with the least RMSE (see Table 3.4 and 3.5).

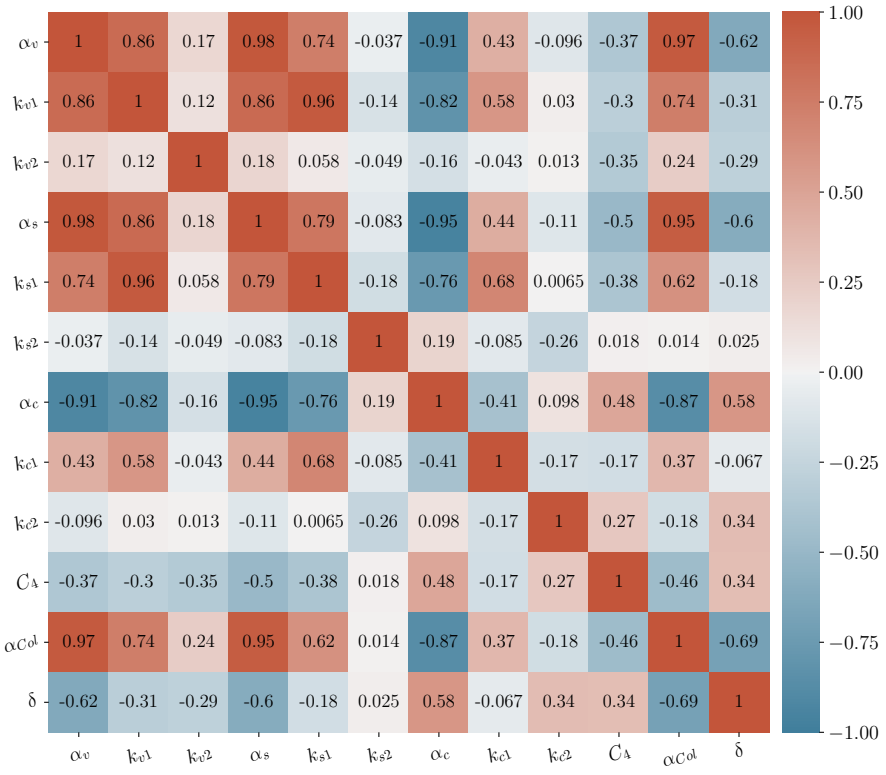

Figure 3.10: The the neutron number N has been plotted against atomic number Z for the stable nuclei the driplines calculated using the modified BW mass formula.

used to constraint the parameters to make a model as accurate as possible. The coefficient of volume energy (α_v) correlate strongly with the k_{v1} while the coefficient of the surface energy (α_s) correlate strongly with the k_{s1}. This imply that the volume and surface energy of a nucleus is influenced by the isospin content of the nucleus. Both α_v and α_s do not correlate with the k_{v2} and k_{s2} respectively indicating their free nature. k_{v2} and k_{s2} represent the I^2 variation of α_v and α_s respectively. These correction in the semi-empirical formula significantly enhances the efficiency of the models. However, they are not easy to constraint experimentally as well. The coefficient of the curvature α_c strongly correlate negatively with the α_v and α_s. Therefore, a stricter assessment of volume and surface coefficients based on experimental findings will be helpful to determine the curvature coefficient and consequently the curvature energy. The curvature energy is important for the accurate estimation of the total surface energy and is often used in the astrophysical calculations. It may be mentioned here that the binding energy is the sum total of all the competing parameters of a mass model in which some parameters can be more significant than other. However, the individual parameters contain important physics and influence the structural effect which are useful in various practical purposes. Therefore, one should carefully select the parameters of the mass model, based on statistical significance as well as the physical implications. The $|I|$ and I^2 dependence of α_c do not correlate with the other model parameters.

Chapter 4

Summary and Future Scope

A simplistic and efficient mass model that addresses the adequate physics of the nucleus and takes the minimalistic computation resources is required in many branches of nuclear physics, such as studying fusion dynamics, decay properties of a nucleus, astrophysical phenomena, etc. In this dissertation, I attempt to optimize the nuclear mass models of the semi-empirical form to estimate the binding energy of nuclei consistent with their experimental/theoretical counterparts. I have fitted the semi-empirical mass formula,by including the various modifications in the latest available experimental mass evaluations and theoretical microscopic evaluation of the Hartree-Fock-Bogoliubov model.It is seen that few modifications in the semi-empirical mass formula yield an efficient mass formula. Among all the modifications, the isospin asymmetry dependence of volume, surface, and curvature coefficients along with the shell energy, plays a predominant role in better estimation of nuclear strength. The isospin asymmetry (I) also plays a significant role in making the model efficient in the lower mass range. The proposed models in this dissertation work excellently well in the medium and higher mass range. Further, the proposed models perform with variable accuracy for different regions of the nuclear mass chart. However, the average performance is at par with the available sophisticated nuclear mass models such as FRDM. A closer inspection of the correlation analysis suggests that the I^2 dependence of the volume, surface, and curvature coefficients does not correlate with the model parameters, making it difficult to constrain the outcome of the concluded result.

The advantage of the form of the semi-empirical formula used in this work is that it has a well-defined temperature dependence of the coefficients in the literature. This will help in extrapolating the fitted formula to the case of finite temperature and thus can be used in various nuclear physics problems such as studying the excited state nuclear dynamics, its multifragmentation, supernova explosion, etc. I have used the formula of Myers and Swiatecki for the shell correction in this work, which can be improved by using

the method of Strutinsky's shell correction or other available methods.

Bibliography

[1] L. Coraggio, S. Pastore, and C. Barbieri, Front. Phys. **8** (2021).

[2] V. Parmar, M. K. Sharma, and S. K. Patra, Phys. Rev. C **105**, 024316 (2022).

[3] S. K. Patra, M. Centelles, X. Viñas, and M. Del Estal, Phys. Rev. C **65**, 044304 (2002).

[4] S. Jain, M. K. Sharma, and R. Kumar, Eur. Phys. J. A **54**, 014102 (2018).

[5] S. Jain, M. K. Sharma, and R. Kumar, Chin. Phys. C. **46**, 014102 (2022).

[6] Y. H. Asres, M. Mathuthu, and Y. A. Ferede, J. Phys. Commun. **3**, 115018 (2019).

[7] Lepine-Szily, A. Lépine-Szily, A. Descouvemont, P. Descouvemont, and Pierre, Int. J. Astrobiol. **11**, 243 (2012).

[8] L. Bonolis, Eur. Phys. J. H . **42** (2017).

[9] A. Burrows, D. Radice, and D. Vartanyan, MNRAS **485**, 3153 (2019).

[10] M. Sneha, M. T. Dulay, and R. N. Zare, Int. J. Mass Spectrom. **418**, 156 (2017).

[11] R. N. Wolf, D. Beck, K. Blaum, C. Böhm, C. Borgmann, M. Breitenfeldt, and Chamel, Phys. Rev. Lett. **110**, 041101 (2013).

[12] A. D. B. Welker A, Althubiti NAS, Phys. Rev. Lett. **110**, 041101 (2017).

[13] S. Beck, B. Kootte, I. Dedes, T. Dickel, A. Kwiatkowski, and E. M. Lykiardopoulou, Phys. Rev. Lett. **127**, 112501 (2021).

[14] W. Huang, M. Wang, F. Kondev, G. Audi, and S. Naimi, Chin. Phys. C. **45**, 030002 (2021).

[15] M. Wang, G. Audi, F. G. Kondev, W. Huang, S. Naimi, and X. Xu, Chin. Phys. C. **41**, 030003 (2017).

[16] V. Parmar, H. C. Das, A. Kumar, M. K. Sharma, and S. K. Patra, Phys. Rev. D **105**, 043017 (2022).

[17] C. v. Weizsäcker, Zeitschrift für Physik **96**, 431 (1935).

[18] W. Pannert, P. Ring, and J. Boguta, Phys. Rev. Lett. **59**, 2420 (1987).

[19] C. Samanta and S. Adhikari, Phys. Rev. C **65**, 037301 (2002).

[20] I. Tews, D. Lonardoni, and S. Gandolfi, Few-Body Syst. **62** (2021).

[21] J. Carlson, Phys. Rev. C **36**, 2026 (1987).

[22] A. A. et al. (ALICE Collaboration), Rev. Mod. Phys. **11**, 811 (2015).

[23] D. Lunney, J. M. Pearson, and C. Thibault, Rev. Mod. Phys. **75**, 1021 (2003).

[24] H. Schatz, L. Bildsten, A. Cumming, and M. Wiescher, Astrophys. J. **524**, 1014 (1999).

[25] R. Baruah, K. Duorah, and H. Duorah, J. Astrophys. Astron. **30**, 165 (2005).

[26] V. Kejzlar, L. Neufcourt, W. Nazarewicz, and P.-G. Reinhard, J. Phys. G: Nucl. Part. Phys. **47**, 094001 (2020).

[27] S. Goriely, N. Chamel, and J. M. Pearson, Phys. Rev. C **82**, 035804 (2010).

[28] J. Mendoza-Temis, J. G. Hirsch, and A. P. Zuker, Nucl. Phys. A **843**, 14 (2010).

[29] P. Möller, A. Sierk, T. Ichikawa, and H. Sagawa, At. Data Nucl. Data Tables **109-110**, 1 (2016).

[30] J. Duflo and A. Zuker, Phys. Rev. C **52**, R23 (1995).

[31] S. Hilaire, M. Girod, S. Goriely, and A. J. Koning, Phys. Rev. C **86**, 064317 (2012).

[32] I. Muntian and Z. Patyk, Phys. Atom. Nuclei **6**, 1051 (2003).

[33] R. Nayak and L. Satpathy, At. Data Nucl. Data Tables **98**, 616 (2012).

[34] X. Tu, H. Xu, M. Wang, Y. Zhang, Y. A. Litvinov, Y. Sun, H. Schatz, X. Zhou, Y. Yuan, J. Xia, et al., Phys. Rev. Lett. **106**, 112501 (2011).

[35] W. D. Myers and W. J. Swiatecki, Nucl. Phys. A **601**, 141 (1996).

[36] H. A. Bethe and R. F. Bacher, Rev. Mod. Phys. **8**, 82 (1936).

[37] W. D. Gunter and R. A. Hubbs, Phys. Rev. **113**, 252 (1959).

[38] M. Bauer and V. Canuto, Nucl. Phy. **72**, 33 (1965).

[39] N. Zeldes, M. Gronau, and A. Lev, Nucl. Phy. **63**, 1 (1965).

[40] W. D. Myers and W. J. Swiatecki, Nucl. Phy. **81**, 1 (1966).

[41] W. D. Myers, At. Data Nucl. Data Tables **17**, 411 (1976).

[42] J. Duflo and A. Zuker, Phys. Rev. C **52**, R23 (1995).

[43] A. Sobiczewski and Y. A. Litvinov, Phys. Rev. C **90**, 017302 (2014).

[44] P. Möller, A. Sierk, T. Ichikawa, and H. Sagawa, At. Data Nucl. Data Tables **109-110**, 1 (2016).

[45] N. Wang and M. Liu, J. Phys. Conf. Ser. **420**, 012057 (2013).

[46] S. A. Sakinah and E. T. Sulistyani, Proc. Int. Conf. Eng. Sci. Appl. **2** (2019).

[47] G. Royer, Nucl. Phys. A **807**, 105 (2008).

[48] K. Pomorski and J. Dudek, Phys. Rev. C **67**, 044316 (2003).

[49] N. Abdelmalek and V. Stavinsky, Nucl. Phy. **58**, 601 (1964).

[50] N. Wang, M. Liu, X. Wu, and J. Meng, Phys. Lett. B . **734**, 215 (2014).

[51] K. Pomorski and J. Dudek, *Nuclear liquid drop model with the surface-curvature terms: New perspectives for the hyperdeformation studies* (2002).

[52] V. Strutinsky, Nucl. Phys. A **95**, 420 (1967).

[53] T. Daniya, D. Kumar, and C. R., Int. J. Control. Autom. **13**, 447 (2020).

[54] P. S. Knopov and A. S. Korkhin, *Regression analysis under a priori parameter restrictions*, vol. 54 (Springer Science & Business Media, 2011).

[55] O. Abiodun, Nature **3**, 382 (1970).

[56] D. N. Basu, Phys. Rev. C **69**, 049803 (2004).

[57] M. Stoitsov, N. Michel, and K. Matsuyanagi, Phys. Rev. C **77**, 054301 (2008).

[58] S. Goriely, M. Samyn, and J. M. Pearson, Phys. Rev. C **75**, 064312 (2007).

[59] M. Samyn, S. Goriely, P.-H. Heenen, J. Pearson, and F. Tondeur, Nucl. Phys. A **700**, 142 (2002).

[60] S. Portnoy and R. Koenker, Statistical Science **12**, 279 (1997).

[61] K. A. e. a. Benzaid D., Bentridi S., Phys. Rev. C **88**, 024308 (2020).

[62] H. Mavromatis, Nucl. Phys. A **162**, 648 (1971).

[63] S. Goriely, N. Chamel, and J. M. Pearson, Phys. Rev. C **88**, 061302 (2013).

[64] S. Goriely and R. Capote, Phys. Rev. C **89**, 054318 (2014).

[65] M. Dahlinger, D. Vermeulen, and K.-H. Schmidt, Nucl. Phys. A **376**, 94 (1982).

[66] G. Audi, A. Wapstra, and C. Thibault, Nucl. Phys. A **729**, 337 (2003).

[67] S. Goriely, N. Chamel, and J. M. Pearson, Phys. Rev. C **88**, 024308 (2013).

[68] V. Parmar, M. K. Sharma, and S. K. Patra, Phys. Rev. C **103**, 055817 (2021).

[69] W. G. Newton, M. Gearheart, and B.-A. Li, Astrophys. J. Suppl. Ser. **204**, 9 (2012).

Turnitin Originality Report

Processed on: 14-Jul-2022 05:27 IST
ID: 1870240587
Word Count: 10336
Submitted: 1

Nitika thesis By Nitika Nitika

Similarity Index	Similarity by Source	
6%	Internet Sources:	3%
	Publications:	4%
	Student Papers:	1%

1% match (publications)
Naz T Jarallah, Murtadha S Nayyef, "Study the Relationship between Beta Decay Stability of Nuclide and its Shape for Some even-even Isobars", Journal of Physics: Conference Series, 2021

< 1% match (publications)
Naz T Jarallah, Murtadha S Nayyef, "Study the Relationship between Beta Decay Stability of Nuclide and its Shape for Some even-even Isobars", Journal of Physics: Conference Series, 2021

< 1% match (Internet from 29-Aug-2021)
https://silo.pub/kernphysik-eine-einfhrung-springer-lehrbuch.html

< 1% match (Internet from 05-Feb-2022)
https://silo.pub/fundamentals-of-probability-with-stochastic-processes-3rd-edition-z-4847565.html

< 1% match (publications)
D. N. BASU, "NEUTRON AND PROTON DRIP LINES USING THE MODIFIED BETHE–WEIZSÄCKER MASS FORMULA", International Journal of Modern Physics E, 2012

< 1% match (publications)
Linn, Khin Nyan, "Structure of exotic nuclei and superheavy elements in meson field theory", Publikationsserver der Goethe-Universität Frankfurt am Main, 2008.

< 1% match (publications)
Alexander Belyaev, Douglas Ross, "The Basics of Nuclear and Particle Physics", Springer Science and Business Media LLC, 2021

< 1% match (Internet from 02-Jan-2022)
https://www.coursehero.com/file/83728431/Nuclear-Reaction-part-2pptx/

< 1% match (Internet from 02-Dec-2020)
https://en.wikipedia.org/wiki/Nuclear_physics

< 1% match (Internet from 10-Sep-2021)
https://iopscience.iop.org/article/10.1088/1674-1137/abddb0

< 1% match (Internet from 28-Jun-2019)
https://aaltodoc.aalto.fi/bitstream/handle/123456789/39076/master_Pham_Phu_2019.pdf?isAllowed=y&sequence=1